

Analysis and Simulation of Magnetically Coupled Y Shape Impedance Source Inverter

C. Bharatiraja*, S. Raghu, Anand Raj and Prabhat kumar

SRM University, Chennai - 603203, Tamil Nadu, India; bharatiraja@gmail.com, raghu.selvaraj89@gmail.com, anandjr994@gmail.com, prabhat0440@gmail.com

Abstract

Objectives: Proposed impedance network also has more degrees of freedom for varying its voltage gain, and hence, improving the versatility of the inverter. A switching algorithm is applied to this topology to control the charging time and discharging interval of inverter inductor. **Methods/Statistical Analysis:** On the basis of the conventional Z-source inverter[ZSI], this paper offer a novel on new type impedance source inverter which only contains one capacitor with tightly coupled three winding transformer, whose obtained voltage gain is presently not matched by existing networks operated at small duty ratio. The inverter can increase the boost factor through adjusting shoot-through duty ratio and varying the number of turns in the three winding transformer. **Findings:** The proposed impedance network also has more degrees of freedom for varying its voltage gain, and hence, improving the versatility of the inverter. A switching algorithm is applied to this topology to control the charging time and discharging interval of inverter inductor. A simple control strategy is applied to this configuration which is responsible for regulating the transfer power to the maximum amount and also to justify the amount of Total Harmonic Dissortion (THD) in minimum point. The working principle of the proposed Y-Source Inverter has been demonstrated by mathematical analysis in detail. The MATLAB/Simulink Simulation results are conducted to validate the analysis. **Application/Improvements:** For regulating the transfer power to the maximum amount in PV applications

Keywords: MATLAB/Simulink, Switching Algorithm, Z-Source Inverter

1. Introduction

Voltage Source Inverters (VSI) and Current Source Inverters (CSI) are two traditional converters which are used conventionally. These traditional converters comprises of six switches fed by source consisting of a battery, fuel cell, solar or any other renewable energy resources. However in the past decade use of a impedance network proven to provide an effective and efficient power conversion between the source and load over a wide range of electric power applications. An impedance network is a combination of inductors and capacitors which acts as a buffer between the converter switches and source

This use of impedance network allows overcoming their common problems like-

Output of the converter can either be great or smaller than the input.

- Main circuits are not interchangeable.
- Vulnerable to the EMI noise in the system.

Various impedance networks are proposed over the past decade, out of which Z-Source¹ impedance is the pioneer and prominent network. It has been used in various DC-DC², DC-AC³, AC-AC⁴ power conversion converters. The voltage fed Z-Source inverter can have high gain theoretically. However, the higher the voltage gain, smaller modulation index has to be used. In applications like fuel cell power conversion, grid integrated Photovoltaic (PV) generation, where a low voltage DC input has to boosted to a higher level AC voltage, smaller modulation index, M will increase the stress on the switches. Thus, networks which can produce higher voltage boost gain at high modulation index are focused. The similar affability has further shown by other impedance networks like quasi-Z⁵, Embedded Z⁶,

*Author for correspondence

series Z⁷, switched inductor⁸, tapped inductor⁹, cascaded¹⁰. However, they add passive components like diode, inductor and capacitor for raising the gain. Increase in components, increases the size of the inverter and is not economically justifiable. Thus the investigation continues with networks using coupled inductors and transformers for boosting the gain. T-Source¹¹, Trans-Z-Source¹², Γ-Source¹³ use coupled inductors or two winding transformer to achieve a higher voltage gain. These networks provide a higher voltage gain while keeping the component count low. These networks have their own characteristic features which might occur depending on the application. It is appropriate to look for an alternative which can combine all the advantages in a single network.

To experience all the preferred characteristics of the various impedance networks (shown in table.1) in a single network, a Y-Source impedance network with a three phase PWM controlled converter is presented in this paper as shown in Figure. 1, which can provide a very high voltage gain while using a small duty ratio with improved flexibility of the network. Proposed Y-source by inverter consists of a DC source, Y-impedance network and a three phase Pulse Width Modulation (PWM) controlled bridge inverter¹⁴. The

Table 1. Comparison of passive components count between different network topologies

Topology	Diode count	Capacitors count	Inductors count
Z-Source [1]	1 Diode	2 Capacitors	2 Inductors
QuasiZ-Source [5]	1 Diode	2 Capacitors	2 Inductors
Γ-Source [13]	1 Diode	2 Capacitors	1 Inductor, 2 winding
TransZ-Source [12]	1 Diode	2 Capacitors	2 integrated 2 winding
Y-source [15]	1 Diode	1 Capacitor	1 integrated winding

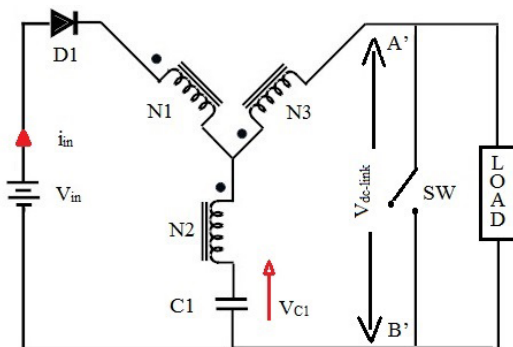


Figure 1. Y-source impedance network.

proposed Y-source network comprises a passive diode D1, a capacitor C1 and a three winding transformer (N1, N2, N3). Since the transformer is directly connected to the Inverter Bridge and diode, effectiveness of the proposed network is ensured by tightening the magnetic coupling between the coupled inductors to avoid the losses through leakage inductances. Bifilar coils¹⁵ may be used to minimize the leakage inductances in the transformer or coupled inductors. Proposed Y-source inverter can realize a very high voltage gain with different winding factor, k, which can be varied by varying the turns ratio (N1:N2:N3) of the three winding transformer. Higher voltage gain is experienced also while using a range of shoot through duty cycle, d_{st} at higher modulation index. Thus the proposed network allows a higher voltage gain with different winding factors, turns ratio and shoot through duty cycle at higher modulation index, which makes the network more versatile and even more flexible than any other present impedance source networks.

Like any other impedance source inverter, Y-source¹⁶ network has a shoot through state, six non-shoot through active states and two zero states. Shoot through operation of the proposed Y-source inverter is discussed in the Section 2. Mathematical analysis of the network is documented in Section 3, control techniques of the inverter is discussed in Section 4, which is validated through simulation in Section 5 and concluded with results.

2. Y-Impedance Inverter Operation

The proposed Y-source impedance operation can be explained with a simple single switch converter as shown in the Figure 2(a). Considering the network working in ideal operating conditions the converter will either be in its shoot-through state or non-shoot-through state while ignoring their leakage inductances¹⁷. For the shoot-through state, switch SW is turned ON to short terminals A' and B', which in turn, causes diode D in the network to reverse bias. The converter is brought back to the non-shoot-through state by turning OFF the switch SW with the diode D conducting. Averaging voltage across the magnetizing inductance¹⁸ for these two states results in the peak dc-link voltage $V_{A'B'}$ across terminals A' and B' in terms of input voltage to the inverter. However this can be achieved only with ideal operating conditions where the leakage inductances of the network is nullified or significantly minimized. Minimization of leakage inductances is not always feasible or cost effective as it requires more

advanced core and windings. Thus effects caused by the leakage inductances must be studied thoroughly.

2.1 Modes of Operation

The proposed Y-source network has a shoot-through and non-shoot-through operation like any other impedance source inverter¹⁹. However, the network undergoes an intermediate third state as explained in this chapter.

2.1.1 Non-Shoot Through to Shoot through Transition

A new intermediate equivalent circuit is introduced when the impedance source transits from non-shoot-through state to shoot through state as shown in Figure 2(a). During non-shoot-through state inductances are all discharging energies and current is thus decreasing. The shunt switch SW in the Figure is next shorted, which ideally, will lead to the shoot-through circuit shown in Figure 2(c). However, for the non-ideal case, an intermediate circuit shown Figure 2(b) will be inserted for a short time interval, caused by the rapid fall of the current through leakage inductance in N1, and rapid rises of currents through leakage inductances N2 and N3. The intermediate state ends only when the leakage current through N1 and diode D falls to zero.

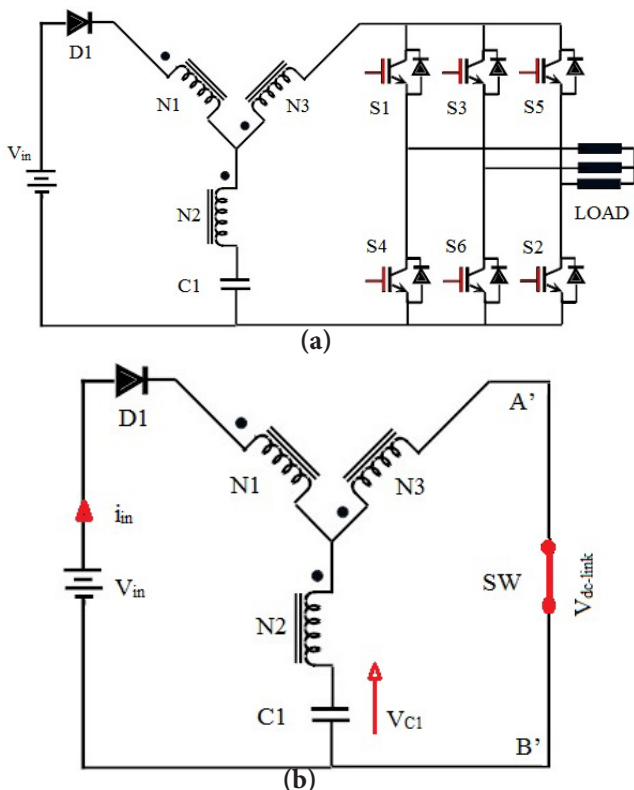


Figure 2. Operation during. (a) Non-shoot through. (b) Intermediate state. (c) Shoot through state.

2.1.2 Shoot through to Non-Shoot through Transition

For shoot through to non-shoot through transition, the network is in its shoot-through state, when the switch SW is turned OFF, the network connects the source to the load and transits to non-shoot through state. Unlike the forward transition, there is no intermediate state and the network enters its non-shoot-through state directly with diode D conducting, even though its current might increase rapidly over a short duration rather than step-increased. No reduction of the shoot-through duration is therefore introduced by the reverse transition. The concern in reverse transition is concentrated on loads, categorized as capacitive and inductive loads, rather than leakage currents.

The first possibility involves the commutation of the network output to a capacitive load. The current drawn by this capacitive load can not adapt to leakage current at instant of commutation, thus voltage spikes²⁰ nor are constraints experienced with capacitive loads. Second possibility involves an inductive load, which may not be as smooth as capacitive load. Being less inductive, during the commutation from shoot through state to non-shoot through state, leakage currents caused by leakage inductance in N3 will be pulled down to output current instantaneously, resulting in high voltage spikes in the circuit. If this transient is not mitigated, it may affect the leakage currents of N1 and N2 as well. Thus a capacitive snubber may be added in order to bring down the difference between the load and leakage currents.

3. Mathematical Analysis

During the shoot through state interval d_{ST} , while the switch SW is ON and diode D1 is reverse biased, the expression for the equivalent circuit is arrived as,

$$V_{C1} + \frac{V_L}{n_{12}} - \frac{V_L}{n_{13}} = 0 \tag{1}$$

Where, $n_{12} = N1/N2$, $n_{13} = N1/N3$ and V_L is given as voltage across winding N1

$$\text{i.e., } V_L = V_{C1} \left(\frac{n_{13} * n_{12}}{n_{12} - n_{13}} \right) \tag{2}$$

On the other hand, during any non-shoot-through state interval $(1-d_{ST})$, diode D1 is conducting and the inverter bridge is conducting source to the load, the expression for the equivalent circuit is arrived as,

$$V_{C1} + V_L + \frac{V_L}{n_{12}} = V_{in} \tag{3}$$

$$\text{i.e., } V_L = [V_{in} - V_{C1}] \left(\frac{n_{12}}{1 + n_{12}} \right) \tag{4}$$

Where V_{C1} is the capacitance voltage

Performing the state-space averaging for both the shoot through state interval and non-shoot through state interval, the voltage across the capacitor C_1 can be deduced to be,

$$V_{C1} \left(\frac{n_{13} * n_{12}}{n_{12} - n_{13}} \right) (d_{ST}) + [V_{in} - V_{C1}] \left(\frac{n_{12}}{n_{12} + 1} \right) (1 - d_{ST}) = 0 \tag{5}$$

From the above expression, the voltage across the capacitor is obtained as

$$V_{C1} = \frac{V_{in} (1 - d_{ST})}{\left[1 - \frac{n_{12} d_{ST} (1 + n_{13})}{(n_{12} - n_{13})} \right]} \tag{6}$$

Referring now to the dc-link voltage across the inverter bridge ($V_{dc-link}$), its peak value $V_{dc-link}$ during the nonshoot through states can be written as

$$V_{dc-link} = V_{in} - V_L + \frac{V_L}{n_{13}} \tag{7}$$

$$V_{dc-link} = \frac{V_{in}}{1 - K d_{ST}} \tag{8}$$

Where
$$k = \left(\frac{N_3 + N_1}{N_3 - N_2} \right), \tag{9}$$

$$N_3 - N_2 > 0, N_1 + 2 N_2 > N_3, N_2 < N_3 \text{ and } N_3 > 1 \tag{10}$$

The Y-source inverter is therefore capable of producing a high gain at a small duty ratio.

$$0 < 1 - K d_{ST} \leq 1 \tag{11}$$

Thus,

$$0 \leq d_{ST} \leq d_{STmax} = 1/k \tag{12}$$

And the corresponding modulation index is

$$M = 1.15 (1 - d_{ST}) \tag{13}$$

The Y-source inverter voltage gain varies with different winding factors K and shoot-through duty cycles d_{ST} . The Equation (8) clearly shows that the Y-source inverter can produce the desired gain with many different combinations of K and d_{ST} . Besides K and d_{ST} the winding turns of the transformer can also be flexibly chosen as long as they give the specified K, which is illustrated in Table 1. Equation (13) depicts that a higher modulation index can be achieved by varying the d_{ST} in the specified range. From Table 1 it can be seen that, for each K value chosen for a certain gain G_v and range for d_{ST} , there are more than one combination of winding turns ($N_1; N_2; N_3$) to select from. In the proposed Y-source inverter²¹, a higher modulation index can be achieved at a small shoot through duty ratio as shown in the Table 1. In this paper, the Y-source network is designed for winding factor 4, which allows shoot through duty ratio between 0 and 1/4, with turns ratio of 1:2:3 as shown in Figure 3. The gain produced by the Y-source network is thus a combination of those expected from the T - or trans-Z-source and Γ -source networks²². This either creates a higher gain or allows merits of the other networks to be flexibly merged. The latter can be helpful when subject to size and type availabilities while choosing magnetic core, wire and coupling method for winding the transformer. The goal is to maximize coupling, and hence minimize leakage, which if not ensured, will lead to higher switching voltage

Table 2. Voltage gain and turns ratio for different

K	$0 < d_{ST} < d_{STmax}$	Voltage Gain, G_v	$N_1:N_2:N_3$
2	$0 \leq d_{ST} \leq 1/2$	$0.5M(1-2d_{ST})^{-1}$	1:1:3, 2:1:4, 1:2:5, 3:1:5
3	$0 \leq d_{ST} \leq 1/3$	$0.5M(1-2d_{ST})^{-1}$	1:1:2, 3:1:3, 2:2:4, 1:3:5
4	$0 \leq d_{ST} \leq 1/4$	$0.5M(1-2d_{ST})^{-1}$	2:1:2, 1:2:3, 5:1:3, 4:2:4
5	$0 \leq d_{ST} \leq 1/5$	$0.5M(1-2d_{ST})^{-1}$	3:1:2, 2:2:3, 1:3:4, 7:1:3
6	$0 \leq d_{ST} \leq 1/6$	$0.5M(1-2d_{ST})^{-1}$	4:1:2, 3:2:3, 2:3:4, 1:4:5

Table 3. Voltage gain of different impedance networks winding factor

Impedance network	Voltage gain, GV
Z-source [1], Quasi Z-source [5]	$0.5M(1-2d_{ST})^{-1}$
T-Source[11], Trans Z-Source [12]	$0.5M(1-(1+n13)d_{ST})^{-1}$
Γ -Source[13]	$0.5M(1-[1+ 1/(n32 -1)] d_{ST})^{-1}$
Y-Source [15]	$0.5M(1- [(1+n13)/(1-n23)] d_{ST})^{-1}$

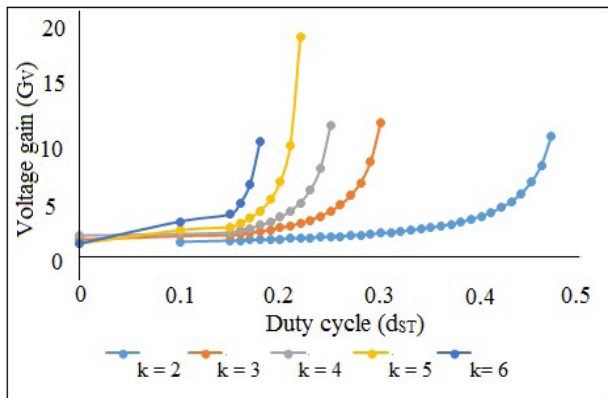


Figure 3. Theoretical gain of inverter for different K and d_{ST}

in addition to a reduction in gain (Table 2. and Table 3). Voltage gain and turns ratio for different and Voltage gain of different impedance networks winding factor.

4. Control Techniques

Pulse Width Modulation (PWM) inversion is an effective technique for increasing power and reducing harmonics of ac waveforms. PWM²¹ control is a common control strategy used in many applications which is the heart of inverter control technique. PWM methods uses high switching frequency carrier waves in comparison to the reference waves to generate a sinusoidal output wave, much like in the two-level PWM case. To reduce harmonic distortions²³ in the output signal phase-shifting techniques are used. Under PWM method, the most popular control technique is the Sinusoidal Pulse Width Modulation (SPWM). Since it has some disadvantages like production of less peak voltage, power transfer etc, it can be rectified with the help of advanced modulation control technique like sine PWM, 60 degree PWM, trapezoidal PWM, stepped wave modulation, switching frequency optimal PWM etc. Double peak PWM is the proposed control

method for the Y-source three phase PWM controlled inverter but can be used with other topologies as well.

The double peak PWM technique is proposed to improve the inverter performance. The Double peak PWM is implemented in the same manner as the SPWM, that is, therefore waveforms are compared with a triangular waveform. As a result, the amplitude of the reference waveforms do not exceed the dc supply voltage $V_{dc}/2$, but the fundamental component is higher than the supply voltage V_{dc} . This is approximately 15.5% higher in amplitude than the normal sinusoidal PWM. Consequently it provides a better utilization of dc voltage. Consider a waveform consisting of a fundamental component with the addition of a triple-frequency term $y = \sin\theta + A\sin3\theta$,

Where $\theta = \omega t$ and A is a parameter to be optimized while keeping the maximum amplitude of $y(t)$ under unity The maximum and minimum of the wave form the reforeoccur at $\cos \theta = (9A-1/12A)^{1/2}$ and $\cos \theta = (1+3A/12A)^{1/2}$

Thus, the double peak sine wave can be obtained from

$$V_{an} = 2/3 (\sin\omega t + 1/6 \sin 3\omega t) \tag{14}$$

$$V_{bn} = 2/3 (\sin(\omega t - 2\pi/3) + 1/6 \sin 3\omega t) \tag{15}$$

$$V_{cn} = 2/3 (\sin(\omega t + 2\pi/3) + 1/6 \sin 3\omega t) \tag{16}$$

With the help of above equations, Double peak PWM waveform has been simulated which is shown in the Figure 4.

5. Results and Discussions

A three phase PWM controlled Y-source inverter is simulated in MATLAB/Simulink platform. The proposed Y-source inverter is simulated with a DC input voltage of 60V while keeping the winding factor, $k = 4$ with winding ratios $N1:N2:N3 = 1:2:3$ at a higher modulation index 0.9 while maintaining the shoot through duty ratio at 0.185 as

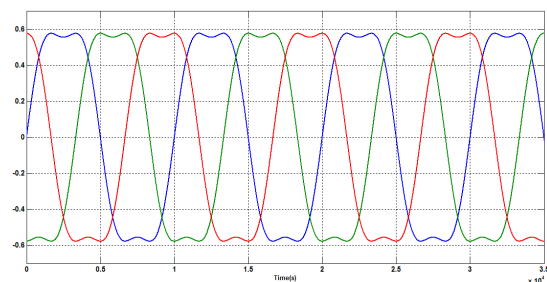


Figure 4. Double peak sine waveform.

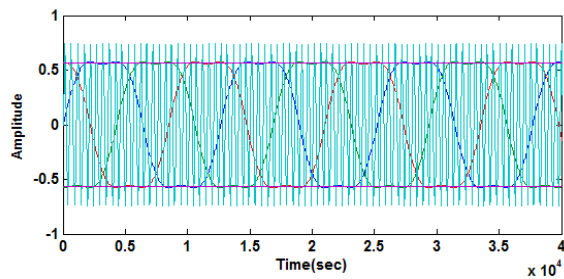


Figure 5. Double peak PWM with shoot through.

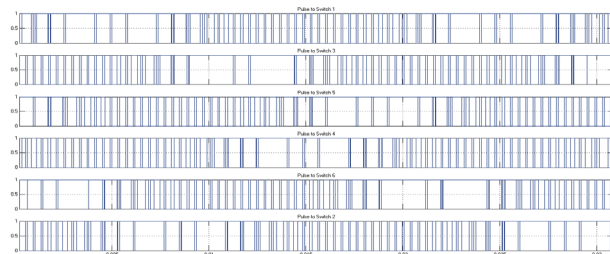


Figure 6. Pulses for inverter.

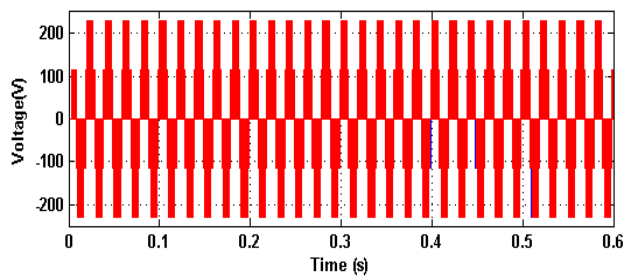


Figure 7. Output voltage waveform for $k = 4$.

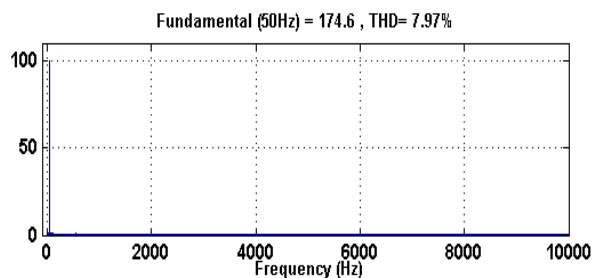


Figure 8. FFT spectrum analysis of output voltage.

shown in Figure 4. The simulation is shown in Figure 5 to 8. Here, the Double peak PWM with shoot through creation carrier and reference waveform is shown in Figure 5, and corresponding PWM is showing in Figure 6. The line voltage waveform and its corresponding harmonics spectrum is shown in Figure 7 and Figure 8.

6. Conclusion

The proposed Y-source inverter can produce a very high voltage gain while operating at a higher modulation index. Voltage gain of different impedance networks in literature has been compared. The flexibility and performance of the proposed inverter are presently unmatched, as it is proved by the mathematical analysis and simulation results. The proposed Y-source inverter operation is better than other impedance source networks and can produce better results for the grid applications and Plug in Hybrid Electric Vehicle [PHEV] applications.

7. References

1. Peng FZ. Z-source inverter. *IEEE Transaction on Industry Application*. 2003 Mar-Apr; 39(2):504–10.
2. Cha H, Peng FZ, Yoo DW. Distributed impedance network (Z network) dc-dc converter. *IEEE Transaction on Power Electronics*. 2010 Nov; 25(11):2722–33.
3. Tang Y, Xie S, Zhang C. Z-source ac-ac converters solving commutation problem. *IEEE Transaction on Power Electronics*. 2007 Nov; 22(6):2146–54.
4. Fang XP, Qian ZM, Peng FZ. Single-phase Z-source PWM ac-ac converters. *IEEE Power Electronics Letter*. 2005 Dec; 3(4):121–4.
5. Anderson J, Peng FZ. Four quasi-Z-source inverters. *Proceeding of IEEE PESC'08; Rhodes, Greece*. 2008 Jun. p. 2743–9.
6. Loh PC, Gao F, Blaabjerg F. Embedded EZ-source inverters. *IEEE Transaction on Industrial Application*. 2010 Jan/Feb; 46(1):256–67.
7. Zhu M, Yu K, Luo FL. Switched inductor Z-source inverter. *IEEE Transaction on Power Electronics*. 2010 Aug; 25(8):2150–8.
8. Nguyen MK, Lim YC, Cho GB. Switched-inductor quasi-Zsource inverter. *IEEE Transaction on Power Electronics*. 2011 Nov; 26(11):3183–91.
9. Zhu M, Li D, Loh PC, Blaabjerg F. Tapped-inductor Z-source inverters with enhanced voltage boost inversion abilities. *Proceeding of IEEE International Conference on Sustainable Energy Technologies; Kandy, Sri Lanka*. 2010 Dec. p. 1–6.
10. Li D, Gao F, Loh PC, Zhu M, Blaabjerg F. Hybrid-source impedance networks: Layouts and generalized cascading concepts. *IEEE Trans Power Electron*. 2011; 26(7):2028–40.
11. Tang Y, Xie S, Zhang C. An improved Z-source inverter. *IEEE Trans Power Electron*. 2011 Dec; 26(12):3865–8.
12. Qian W, Peng FZ, Cha H. Trans-Z-source inverters. *IEEE Trans Power Electron*. 2011 Dec; 26(12):3453–63.

13. Loh PC, Li D, Blaabjerg F. T-Z-source inverters. *IEEE Trans Power Electron.* 2013 Nov; 28(2):4880–4.
14. Bifilar Coil. Available from: http://en.wikipedia.org/wiki/Bifilar_coil
15. Siwakoti YP, Loh PC, Blaabjergand GF. Town, Y-source impedance network. *Proceeding of APEC 2014; Fort Worth, TX.* 2014 Mar. p. 3362–6.
16. Prakash G, Subramani C. Modulation and analysis of quasi z-source inverter for solar photovoltaic system. *Indian Journal of Science and Technology.* 2016 May; 9(19):1–7.
17. Sivapriyan R, Umashankar S. Comparative analysis of PWM controlling techniques of single phase Z-source inverter. *Indian Journal of Science and Technology.* 2016 Jul; 9(26):1–5.
18. Kamalakkannan S, Kirubakaran D. Maximum Power Point Tracking (MPPT) for a PV powered Z-source inverter. *Indian Journal of Science and Technology.* 2016 Jul; 9(28):1–8.
19. Bharatiraja C, Jeevananthan S, Latha SR, Mohan V. Vector selection approach-based hexagonal hysteresis space vector current controller for a three phase diode clamped MLI with capacitor voltage balancing. *IET Power Electron.* 2016 Jun; 9(7):1350–61.
20. Bharatiraja C, Jeevananthan S, Munda JL, Latha R. Improved SVPWM vector selection approaches in OVM region to reduce common-mode voltage for three-level neutral point clamped inverter. *International Journal of Electrical Power and Energy Systems.* 2014 Oct; 79(1):285–97.
21. Bharatiraja C, Jeevananthan S, Latha R. FPGA based practical implementation of NPC-MLI with SVPWM for an autonomous operation PV system with capacitor balancing. *International Journal of Electrical Power and Energy Systems.* 2014 Oct; 61(1):489–509.
22. Bharatiraja C, Munda JL. Simplified SVPWM for Z source T-NPC-MLI including neutral point balancing. 4th IEEE Symposium on Computer Applications and Industrial Electronics (ISCAIE2016); Malaysia. 2016.
23. Prakash G, Subramani C, Bharatiraja C, Shabin M. A low cost single phase grid connected reduced switch PV inverter based on time frame switching scheme. *International Journal of Electrical Power and Energy Systems.* 2016 Mar; 77:100–11.